Theor Appl Genet (2012) 125:1125–1135
DOI 10.1007/s00122-012-1899-2

ORIGINAL PAPER

Characterization, fine mapping and expression profiling of *Ragged leaves1* in maize

Haiying Guan · Chaoxian Liu · Yuanzeng Zhao · Biao Zeng · Hainan Zhao · Yi Jiang · Weibin Song · Jinsheng Lai

Received: 4 January 2012 / Accepted: 11 May 2012 / Published online: 31 May 2012

Abstract The *Ragged leaves1* (*Rg1*) maize mutant frequently develops lesions on leaves, leaf sheaths, and ear bracts. Lesion formation is independent of biotic stress. High-level accumulation of H_2O_2 revealed by staining *Rg1* leaves, with 3′,3′-diaminobenzidine and trypan blue, suggested that lesion formation appeared to be due to cell death. *Rg1* was initially mapped to an interval around 70.5 Mb in bin 3.04 on the short arm of chromosome 3. Utilizing 15 newly developed markers, *Rg1* was delimitated to an interval around 17 kb using 16,356 individuals of a BC1 segregating population. There was only one gene, *rp3*, predicted in this region according to the B73 genome. Analysis of transcriptome data revealed that 441 genes significantly up-regulated in *Rg1* leaves were functionally over-represented. Among those genes, several were involved in the production of reactive oxygen species (ROS). Our results suggested that lesions of *Rg1* maize arose probably due to an aberrant rust resistance allele of *Rp3*, which elicited the accumulation of ROS independent of biotic stress.

Communicated by T. Luebberstedt.

Haiying Guan and Chaoxian Liu contributed equally to this work.

Electronic supplementary material The online version of this article (doi:10.1007/s00122-012-1899-2) contains supplementary material, which is available to authorized users.

H. Guan · C. Liu · B. Zeng · H. Zhao · Y. Jiang · W. Song · J. Lai (✉)
Department of Plant Genetics and Breeding, State Key Laboratory of Agrobiotechnology and National Maize Improvement Center of China, China Agricultural University, Beijing 100193, China
e-mail: jlai@cau.edu.cn

Y. Zhao
Department of Life Science and Technology, Henan Institute of Science and Technology, XinXiang 453003, China

Introduction

Plant mutants that spontaneously develop patches of dead cells in the absence of stress, pathogen attack or injury are defined as lesion-mimic mutants, because their phenotypes are similar to disease symptoms or pathogen-induced hypersensitive response (HR) cell death. These mutants were first reported in maize (Hoisington et al. 1982) and later in many other plants, including barley (Rostoks et al. 2006; Wolter et al. 1993), *Arabidopsis* (Dietrich et al. 1994; Greenberg and Ausubel 1993; Greenberg et al. 1994), rice (Mori et al. 2007; Qiao et al. 2010; Wu et al. 2008), and wheat (Li and Bai 2009; Yao et al. 2009). These mutants, particularly those with HR (Lorrain et al. 2003), are important tools for dissecting the genetics of programmed cell death (PCD) in plants. In recent years, studies in a variety of plants suggested that the lesions produced by lesion-mimic mutants resemble HR, because of the involvement of disease-resistance and defense-related genes in the formation of lesions (Johal et al. 1995). A number of lesion-mimic alleles have been cloned and characterized, including *spl11*, *spl7, Spl18*, and *Spl28* in rice (Zeng et al. 2004; Yamanouchi et al. 2002; Mori et al. 2007; Qiao et al. 2010); *mlo* and *nec1* in barley (Wolter et al. 1993; Rostoks et al. 2006); and *Les22* and *Lls1* in maize (Hu et al. 1998; Gray et al. 1997).

In maize, except to lesion-mimic mutants that have already been cloned, the mechanisms of lesion formation for several lesion-mimic mutants remain largely unknown. For example, *Rg1*, which was initially identified from a

single plant growing in a block of sweet corn hybrids at the Agricultural Experiment Station in Madison, Wisconsin in 1927, frequently causes "spontaneous" necrosis on leaves, leaf sheaths, and ear bracts, which resembles the lesion-mimic phenotype. Brink and Senn (1931) first reported that *Rg1* was controlled by a single dominant gene and linked with *tassel seed4* and *dwarf5* located on maize chromosome 3; *Rg1* lesions occur not only on the leaf blades, but also on the leaf sheaths and ear bracts, while the roots and stems of *Rg1* plants show no developmental or anatomical differences from the control. Lesions formation results from cytolysis of mesophyll cells (Mericle 1950). Bongard-Pierce et al. (1996) found that the appearance of these lesions was correlated with the loss of epicuticular wax. In a small population of 427 individuals, *Rg1* was found to be completely linked with *Rp3*, which conditions race-specific resistance to *Puccinia sorghi* (Sanz-Alferezet al.1995). The *Rp3* locus is a complex locus at which at least six different haplotypes occur (*Rp3A–Rp3F*) conferring different resistance specificities to eight *Puccinia sorghi* biotypes (Wilkinson and Hooker 1968). In most *Rp3*-carrying lines, the locus was composed of at least nine nucleotide-binding site-leucine rich repeat (NBS-LRR) gene family members (Webb et al.2002). In this study, the phenotype of the *Rg1* was further characterized. A high-resolution genetic map was constructed using a large BC1 segregating population. Finally, the *Rg1* was delimitated to a small interval (17 kb in the reference B73 genome). There was only one gene, (*Rp3*) predicted in this region in B73 genome suggesting *Rg1* was likely a novel *Rp3* allele. Transcriptome analysis revealed that *Rg1* triggered the accumulation of ROS, which then induced HR including, the up-regulation of defense-related genes and the production of antimicrobial compounds.

Materials and methods

Plant materials and growth conditions

The *Rg1* mutant was obtained from the Maize Genetics Cooperation Stock Center. For fine mapping, the *Rg1* mutant was grown at Shang Zhuang Experimental Station of China Agricultural University for phenotype observation. It was back-crossed one or more times into a B73 genetic background to generate a backcross population.

A BC3 segregating population was grown to determine when the lesion-mimic phenotype appeared and whether lesions in *Rg1* mutants formed independent of biotic stress under aseptic conditions. BC3 segregating population seeds were sterilized with 20 % bleach for 30 min, rinsed three times in sterile water, and germinated on MS0 medium containing 0.3 % phytagel in an autoclaved glass bottle. Plants were grown until lesions formed in a greenhouse with a temperature range from 22 °C (night) to 28 °C (day) and 16-h light/8-h dark (Yin et al. 2000).

Scanning electron microscopy

The BC3 segregating population was grown in a climate chamber. When the fourth leaf was not fully expanded, but the lesions emerged, the fourth leaf was excised from *Rg1* and the control plants and immediately observed under scanning electron microscopy (TM3000, Hitachi) to determine the number and morphology of stoma in the epidermis.

Histochemical analysis

Leaves for 3′,3′-diaminobenzidine (DAB) and trypan blue staining were collected from a BC3 segregating population grown for 3 weeks. Hydrogen peroxide was detected using the DAB staining method as described previously with some modification (Li et al. 2005). Five centimeter leaf sections were excised from the fourth leaf of each plant. The cut ends of the leaves were immersed in water with DAB at 1 mg/ml and adjusted to pH 3.8 to dissolve the DAB. Leaves were then incubated in the growth chamber for an additional 8-h period to allow DAB uptake and reaction with H_2O_2 and peroxidase. For fixation, 3-cm segments cut from the center of inoculated leaves were bleached in 75 % ethanol and then heated for 10 min. The leaf segments were afterward transferred into 50 % glycerol for storage or 10 % glycerol for microscopic analysis. Trypan blue staining was done as previously described (Bowling et al. 1997). Briefly, leaves were submerged in trypan blue solution (2.5 mg/ml of trypan blue, 25 % [w/v] lactic acid, 23 % water-saturated phenol, 25 % glycerol) at 70 °C and infiltrated for 10 min, then heated in boiling water for 2 min, and left to stain overnight. After destaining in a chloral hydrate solution (25 g in 10 ml of H_2O) for 3 days, samples were equilibrated with 70 % glycerol for microscopic analysis (Yin et al. 2000). Samples were observed under a dissecting microscope (Olympus, SZX16-DP72).

DNA extraction

Genomic DNA was extracted from leaves of 3-week-old plants by the CTAB method (Saghai-Maroof et al. 1984). Genomic DNA from seeds was isolated by the following method: endosperm the size of a sesame seed was cut from the apex of the seeds and boiled with 100 µl 0.1 mol/L NaOH for 10 min at 100 °C in a thermal cycler. Then 100 µl of TE (pH 2.0) was added and the mixture was centrifuged at 2,000 rpm (Eppendorf) for 2 min at room

temperature. The supernatant was used as the template for genotype analysis.

Marker development and gene prediction

Simple sequence repeats (SSR) were searched by SSR-Hunter1.3 (Li and Wan 2005) and BLAST against the high throughput genomic sequences (HTGS) database of maize (http://blast.ncbi.nlm.nih.gov/Blast.cgi?PROGRAM=blastn&BLAST_PROGRAMS=megaBlast&PAGE_TYPE=BlastSearch&SHOW_DEFAULTS=on&LINK_LOC=blasthome) for picking unique sequences. Primers flanking microsatellite repeats were designed by Primer Premier 5.0 (Palo Alto, CA) and tested by polymerase chain reaction (PCR) amplification using DNA from the parents. The amplification products were run on 6 % denaturing polyacrylamide gels for polymorphism tests. In addition to the development of SSR markers, indel polymorphism (IDP), and cleaved amplified polymorphic sequence (CAPS) markers were also developed using single-copy DNA segments with allelic diversity. The unique sequences with insertion or deletion between parents were used to develop IDP markers, and the unique sequences with single-nucleotide polymorphism (SNP) diversities were utilized to develop CAPS markers by SNP2CAPS (Thiel et al. 2004). The gene prediction was conducted by Softberry (http://linux1.softberry.com/berry.phtml?topic=fgenesh&group=programs&subgroup=gfind).

Transcriptome sequencing and gene annotation

The BC3 segregating population was grown in a greenhouse. When the plants had eight leaves, total RNA was extracted (RNAprep pure Plant Kit, TIANGEN) from the eighth leaves of ten *Rg1* plants and ten wild-type siblings, respectively, and used for Illumina sequencing.

The sequencing reads were aligned and assembled using TopHat v.1.3.1 and Cufflinks v.1.0.2, respectively, and the B73 5b genome was used as a reference sequence. Comparison with a reference GTF annotation file was performed using Cuffcompare, when all short read sequences were assembled with Cufflinks v.1.0.2. Cuffdiff was used to identify genes with differential expression by tracking changes in the relative abundance of genes in different samples. Differentially expressed genes were determined by using two cutoffs: statistical significance of $p < 0.05$ and a three-fold change in gene expression. Over-expressed genes were assigned into different categories according to their functions in biological process, cellular component, and molecular function compared with the corresponding functional categories of all the genes in maize (http://bioinfo.cau.edu.cn/agriGO/analysis.php) finally, the over-represented genes were obtained (p value and false discovery rate <0.05).

Semi-quantitative RT-PCR

To validate the transcriptome sequencing data, primers for amplifying randomly selected defense-related genes for semi-quantitative RT-PCR were designed. Of the seven primers, five were designed by us. The two for GRMZM2G028393 and GRMZM2G156632 came from previous studies (Chintamanani et al. 2010; Feng et al. 2007).

Results

Characterization of the *Rg1* mutant

The maize elite inbred line B73 used as the recurrent parent was crossed to *Rg1* mutant to generate the backcross population. At the seedling stage, almost none of the *Rg1* plants with two to three leaves in the BC3 segregating population could be distinguished from wild-type siblings. The emergence of lesions was generally first visible on the fourth leaf of the heterozygous plants, both in the field and in the greenhouse (Fig. 1a). These lesions were initially confined to the small local regions and gradually enlarged; eventually, the whole leaf blades became a mosaic of dead and live areas (Fig. 1b–d). Scanning electron microscopy was used to carefully observe the difference between *Rg1* necrosis areas and wild-type leaves. The epidermal cells from necrosis areas of *Rg1* plants appeared small with smooth outlines, and the epidermis lacked stomata (Fig. 1e, f). Lesions not only occurred on the leaf blades, but also appeared on the leaf sheaths and ear bracts (Fig. 1g–j). Lesions on the leaf sheaths did not seem as severe as those on the leaf blades.

In addition to the effects of *Rg1* on the leaf blades, leaf sheaths, and ear bracts, the architecture of plants was also affected. In the BC3 segregating population, it was clear that heterozygous *Rg1* plants were thinner and shorter than wild-type siblings. Most of the *Rg1/rg1* plants could produce viable pollen and seeds, and only a few heterozygous *Rg1* plants could not produce normal tassels and ears.

To determine whether lesions in *Rg1* mutants formed independent of biotic stress, both normal plants and heterozygous *Rg1* mutants from the BC3 segregating family were grown under sterile conditions. The emergence of lesions showed no apparent difference from those plants grown in the greenhouse (data not shown). The results strongly confirmed that lesion formation in the *Rg1* mutants was independent of biotic stresses. The leaves taken from 3-week-old mutants and their wild-type siblings were stained with DAB, an indicator for high-level H_2O_2. As shown in Fig. 1k, l, brownish precipitates were only observed in the *Rg1* leaves. These results suggested

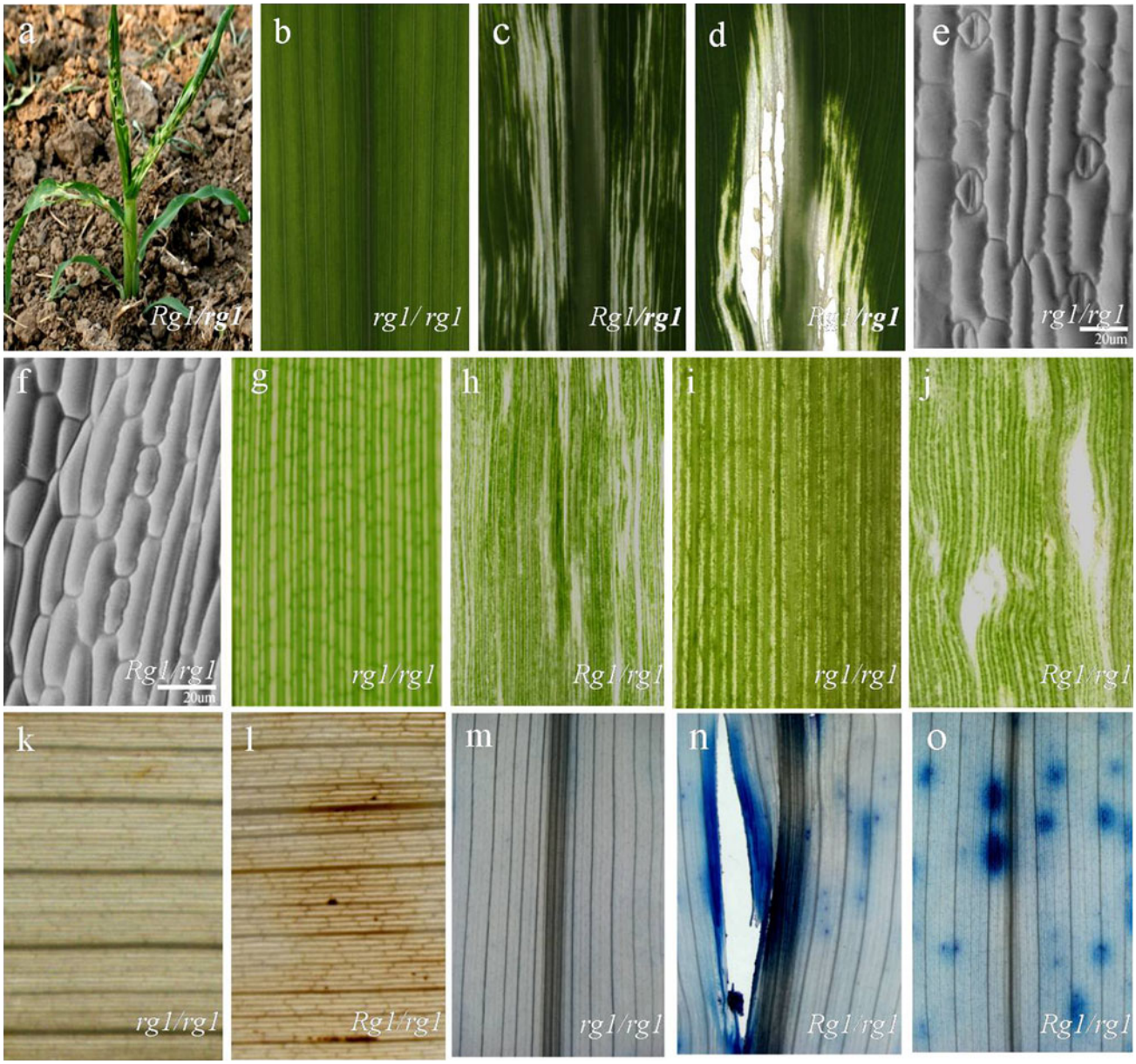

Fig. 1 Phenotypic analysis of heterozygous *Rg1* plants and its wild-type siblings. **a** Phenotypic observation of heterozygous *Rg1* plants grown at Shang Zhuang Experimental Station in Beijing for 3 weeks. **b** Phenotypic observation of wild-type leaves. **c**, **d** Phenotypic observation of the ragged leaves of *Rg1* plants. **e**, **f** Stomata observation of the fourth leaves of wild-type and *Rg1* plants under scanning electron microscopy. **g**, **h** Phenotypic observation of leave sheaths of wild-type and *Rg1* plants under a dissecting microscope. **i**, **j** Phenotypic observation of ear bracts of wild-type and *Rg1* plants under a dissecting microscope. **k**, **l** DAB staining of developing *Rg1* leaves and its wild-type siblings. **m** Trypan blue staining of wild-type leaves. **n**, **o** Trypan blue staining of *Rg1* leaves

that a high level of H_2O_2 accumulated in the *Rg1* leaves. Leaves of *Rg1* plants and their wild-type siblings were also stained with trypan blue, a histochemical indicator of irreversible membrane damage or cell death. On the surface of *Rg1* leaves with large tears, deep blue staining was localized on the edges of the necrotic lesions (Fig. 1n) but also occurred in "normal" areas, where cells may have been dying, but were too small to be observed by the unaided eye (Fig. 1o). No area was stained blue in the control (Fig. 1m).

Genetic analysis and preliminary mapping of the *Rg1*

The BC1 population segregated for 1,800 *Rg1* mutants and 1,803 wild-type plants, and these numbers fell within the statistical limits of the expected 1:1 pattern ($\chi^2 = 0.0025$).

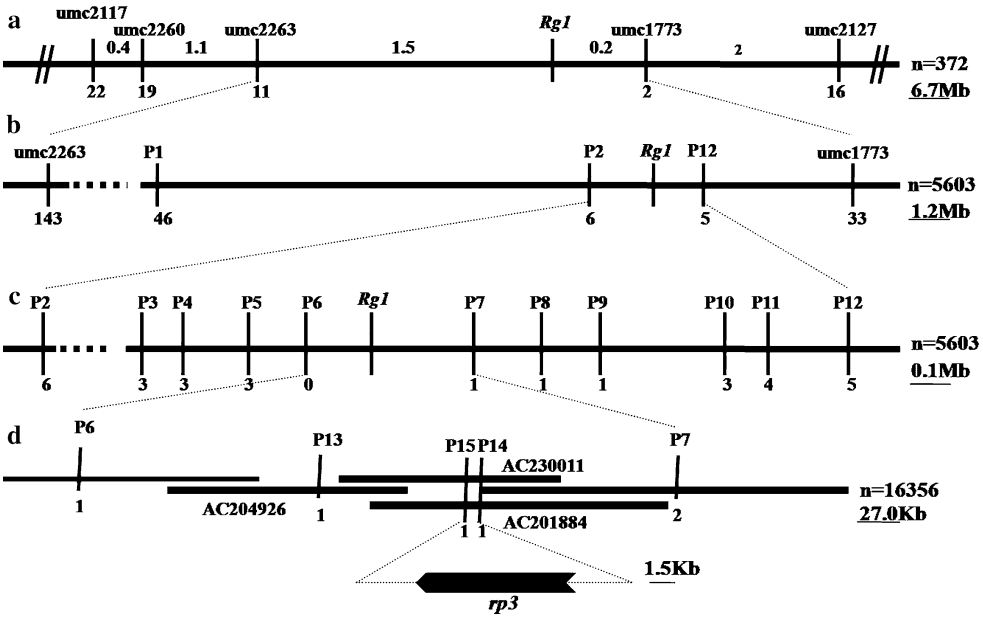

Fig. 2 Fine mapping of *Rg1*. **a** The *Rg1* locus was delimited to an interval flanked by umc2263 and umc1773 on the short arm of chromosome 3 using 372 *Rg1* individuals of BC1. **b**, **c** Fine mapping of the *Rg1* locus using 5,603 individuals of BC1. d.The *Rg1* locus was finally delimited to an around 17-kb interval flanked by P14 and P15 in B73 genome using 16,356 individuals, the candidate region was located on AC230011 Chromosome 3. The *numbers below and above the horizontal line*, respectively, represent recombinational events and genetic distance (cM). The *scale bar* represents the real physical distance

The phenotypic segregating ratio suggested that the *Rg1* character was governed by a single dominant gene, which was in agreement with the original research (Brink and Senn 1931). *Rg1* was first reported to be located on chromosome 3 (Brink and Senn 1931), and it was later mapped to bin 3.04 (Maize GDB, IBM2 2008 Neighbors).

Preliminary mapping of *Rg1* was conducted using BC1 segregating population. A total of 43 SSR core markers available from the public database on maize GDB in the bin3.04–3.05 on maize chromosome 3 were screened by polyacrylamide gel electrophoresis. Five SSR markers had genetic polymorphisms between *Rg1* and B73. The two markers, umc2117 and umc2127, were first used to screen the 372 *Rg1* plants of the BC1 segregating population, and 38 recombinants combined with phenotypes indicated the loci of *Rg1* was between marker umc2117 and umc2127. Other three markers, umc2260, umc2263 and umc1773, were also used to screen the 38 recombinants, and *Rg1* was mapped to a 1.7-cM region between umc2263 and umc1773 in bin 3.04, which is the centromeric region of chromosome 3 (Farkhari et al. 2011). The physical distance between markers umc2263 and umc1773 is about 70.5 Mb, according to the reported B73 whole genome sequence (Fig. 2a).

Fine mapping of *Rg1*

To determine the precise position of *Rg1*, eight SSR markers, two CAPS markers, and five IDP markers with genetic polymorphisms between two parents were newly developed (Table 1). Meanwhile, a large BC1 segregating population consisting of 5,603 plants was used to obtain more plants with crossovers. A total of 143 and 33 recombinants were screened out by umc2263 and umc1773, respectively, and were further analyzed by the newly developed markers. *Rg1* was mapped to a region about 600 kb between marker P5 and P7 (Fig. 2b, c). No recombinant was detected between marker P6 and *Rg1*, suggesting that this marker was closely linked to *Rg1*. To further narrow down the *Rg1* locus, 10,752 seeds of the BC1 segregating population were screened, and *Rg1* was finally delimited to a region of 17 kb of the B73 genome flanked by marker P15 and P14 (Fig. 2d), while the corresponding region in the *Rg1* line was probably at least 50 kb.

Gene prediction was conducted on the 17-kb region of the B73 genome. The only one predicted gene in this region encoded a putative rust resistance protein rp3. In *Rg1* mutant, the corresponding region was a complex locus probably containing multiple *Rp3* alleles. It is likely that a novel *Rp3* allele possibly generated by an intragenic recombination event underlies the *Rg1* phenotype.

Transcriptome analysis

Transcriptome sequencing have resulted in a total of 21,074,174 and 21,201,466 reads of 100 base pairs from *Rg1* leaves and the control plants, respectively. The sequencing reads were mapped on the B73 genome, covering 17,828 and 17,466 genes in the *Rg1* leaves and the control, respectively.

Differentially expressed genes were determined by using two cutoffs: statistical significance of $p < 0.05$ and a threefold change in gene expression. A total of 830 and 65

Table 1 Newly developed markers used for fine mapping of *Rg1*

Physical location (Mb)	BAC accession number	Marker	Forward primer (5′–3′)	Reverse primer (5′–3′)	Type	Product size (bp)	Restriction enzymes
99.2	AC207816.4	P1	CAGCCTCATCCCTCATGCTC	GGTTTCTCCTGGCCCTTCA	SSR	256	
112	AC216864.3	P2	AAGAGGATGATGACGGACAGG	TGCCGTATAGCAAGCAGAGC	SSR	268	
113.2	AC190622.1	P3	CGCTCACAACACTCCAAC	TAGCCTACCCCAACTTCC	SSR	178	
113.3	AC185252.4	P4	GCAAAGGAATGGACAAGT	TGGGAAAAACAAAGGCAG	SSR	178	
113.5	AC194302.3	P5	ATCCAGGCAACAAGACGA	GGAGTAGGAGGGAACAACAT	CAPS	569	TaqI
113.6	AC213856.4	P6	CCTATGGTGGAGGTCAAG	TGTGAGGCAATGGAAAG	IDP	153	
114.1	AC197777.3	P7	TTCTATGAAGTATTCCCTCCG	TTCTATGAAGTATTCCCTCCG	IDP	748	
114.3	AC190513.1	P8	CAAAGTGTTTGGTTTGGTAGC	AGATGTATTTGCACAAGAGGC	IDP	238	
114.5	AC207336.2	P9	GTTTACCATGCTCACGTCTGATTAA	CATCTCCTACCTTGAGTCCCTGC	SSR	260	
114.8	AC207414.3	P10	ACGGCGTTGCGTGGTCT	GTGCCATGTGGTTAGATGGATAA	SSR	155	
114.9	AC220955.3	P11	TTGAGATGGTGAGGGAGC	TTGATTTGGAATGCGACA	SSR	149	
115	AC210189.3	P12	GTTCACCACCGCCATCAC	CGCAAGACAAAGCACTCC	SSR	186	
113.8	AC204926.3	P13	AACTAACTTTAACCATAATTGG	GCTGAGCCAAGCATATT	IDP	139	
114	AC230011.2	P14	CGATGGCGATTTCTGACG	TGGGCTCAAGGAATGAAGG	CAPS	999	RsaI
114	AC230011.2	P15	CTGTCTCGAGTGGGGTGTCT	ACTTGTTCCAATTTGGTGCTT	IDP	1,222	

genes were shown to be significantly up-regulated and down-regulated in *Rg1* leaves compared with the control, respectively (Supplementary material: Table S1–S4). When assigned the 830 up-regulated genes into different functional categories and compared with the number of all genes in maize genome of the corresponding functional categories, 441 genes belonging to 58 categories were shown to be over-represented (Table S5, S6). These 441 genes were called "over-represented" genes. Most of the over-represented genes have functions related to catalytic activity (16.72 %), followed by transferase activity (6.4 %) and oxidoreductase activity (4.15 %).

Among the 441 over-represented genes, *NADPH oxidase*, *peroxidase*, and *polyamine oxidase* are significantly up-regulated with fold changes ranging from 3.29 to 6.12. One *peroxidase* (GRMZM2G061230) is exclusively expressed in *Rg1* leaves. It has been reported that *NADPH oxidase*, *peroxidase*, and *polyamine oxidase* functioned in the production of ROS (Mittler et al. 2004). Proteins involving in the production of ROS are typically localized at plasma membrane (such as *NADPH oxidase*) or apoplast (such as *peroxidase* and *polyamine oxidase*) (Daudi et al. 2012; Sebela et al. 2001). The sub-cellular localization of the highly up-regulated *NADPH oxidase*, *peroxidase*, and *polyamine oxidase* is therefore predicted by ProtComp Version 9.0 (comprehensive score of more than 9.0). The results show that 1 of the 2 up-regulated *polyamine oxidases* and 6 of 16 up-regulated *peroxidases* are predicted to be in the apoplast, and the up-regulated *NADPH oxidase* is predicted to be in plasma membrane. Therefore, we consider that these genes probably participate in the production of ROS (Table 2).

Among the 441 over-represented genes, there are also a set of genes related to defense response, including *beta-1,3 glucanase*, *chitinase*, *protease inhibitor, rust resistance kinase Lr10*, *pathogenesis-related protein class1*, and *dehydrin* (Table 2). The fold change of these genes ranges from 4.67 to 31.79. There are three *chitinase* (GRMZM2G 358153, GRMZM2G005633, GRMZM2G051921) and one *wound-induced serine protease inhibitor1* (GRMZM2G15 6632), exclusively expressed in *Rg1* leaves. It is worthwhile to note that *dehydrin*, a gene frequently reported to be induced by abiotic stress, is up-regulated to 31.26-fold in *Rg1* leaves as compared to wild type.

Additionally, a group of genes encoding key enzymes involved in the phenylpropanoid pathway are also over-represented (Table 2). These genes had expression level of 3.4- to 7.11-fold more in *Rg1* leaves than in that of wild-type plants. One such enzyme, laccase (GRMZM2G3363 37), is exclusively expressed in *Rg1* leaves.

To validate the results of transcriptome sequencing, primers were designed for semi-quantitative RT-PCR to amplify randomly selected defense-responsive genes (Table 3). It had previously been reported that *PLD* (*phospholipase D*), *LOX* (*lipoxygenase*), *chitinases*, *JIP* (*jasmonate-induced protein*), *peroxidase3*, *WIP1* (*wound-induced serine protease inhibitor1*), and *MPI* (*maize proteinase inhibitor*) were involved in response to biotic stress (Kawano 2003; Rohrmeier and Lehle 1993; Sandhu et al. 2007; Schweizer et al. 1997; Van Der Luit et al. 2000;

Table 2 Over-represented genes associated with the production of ROS, defense response, and phenylpropanoid pathway in *Rg1* leaves

Gene ID	Annotation	FDR	Fold change	Sub-cellular localization
Genes related to production of ROS				
GRMZM2G341934	Peroxidase	0.00008	3.29	Apoplast
GRMZM2G061230	Peroxidase	0.00008	a	Apoplast
GRMZM2G126261	Peroxidase	0.00018	6.12	Apoplast
GRMZM2G122853	Peroxidase 1	0.00018	5.36	Apoplast
GRMZM2G135108	Peroxidase	0.00018	3.80	Apoplast
GRMZM2G450233	Peroxidase	0.00018	5.08	Apoplast
GRMZM2G441541	NADPH oxidase	0.00018	4.41	Plasma membrane
GRMZM2G071343	Polyamine oxidase	0.00018	5.61	Apoplast
Genes related to defense response				
GRMZM2G125032	Beta-1,3-glucanase precursor	0.0000082	29.08	
GRMZM2G431039	Putative beta-1,3-glucanase	0.0000082	8.30	
GRMZM2G065585	Beta-1,3 glucanase	0.0000082	16.57	
GRMZM2G129189	Class iv chitinase	0.0000082	5.31	
GRMZM2G162359	Class iii chitinase homolog	0.0000082	9.39	
GRMZM2G358153	Chitinase 1	0.0000082	a	
GRMZM2G005633	Chitinase	0.0000082	a	
GRMZM2G051921	Chitinase	0.0000082	a	
GRMZM2G051943	Chitinase	0.0000082	15.14	
GRMZM2G145518	Chitinase	0.0000082	21.80	
GRMZM2G156632	Wound-induced serine protease inhibitor	0.00008	a	
GRMZM2G075315	Bowman–Birk type trypsin inhibitor	0.00008	20.94	
GRMZM2G055802	Bowman–Birk type trypsin inhibitor	0.00008	10.42	
GRMZM2G465226	Pathogenesis-related protein class 1	0.00008	4.67	
GRMZM2G079440	Dehydrin7	0.0094	31.26	
GRMZM2G373522	Dehydrin cor410	0.0094	9.96	
GRMZM2G079219	Rust resistance kinase Lr10	0.00018	9.35	
GRMZM2G034611	Rust resistance kinase Lr10	0.00018	11.82	
GRMZM2G077914	Rust resistance kinase Lr10	0.00018	12.58	
GRMZM2G113421	Rust resistance kinase Lr10	0.00018	31.79	
Genes involving in the phenylpropanoid pathway				
GRMZM2G081582	Phenylalanine ammonia-lyase	0.00018	3.43	
GRMZM2G127948	Caffeoyl-CoA O-methyltransferase	0.00018	3.70	
GRMZM2G147245	Cinnamate-4-hydroxylase	0.00018	3.80	
AC210173.4_FG005	Ferulate-5-hydroxylase	0.00018	5.52	
GRMZM2G336337	Laccase	0.00008	a	
GRMZM2G090087	Aldehyde dehydrogenase	0.00018	3.40	
GRMZM2G124365	Chorismate mutase	0.00018	7.11	

Fold change indicates those genes were significantly up-regulated more than threefold in *Rg1* leaves compared to its wild-type siblings

FDR false discovery rate

[a] Indicates the genes exclusively expressed in *Rg1* leaves

Xu et al. 2007). As shown in Fig. 3, these genes showed the same expression profiling with the transcriptome sequencing. *Chitinase*, *JIP,* and *WIP1* were specifically activated; *PLD*, *LOX*, *MPI,* and *peroxidase 3* were predominantly activated in *Rg1* plants compared with wild-type siblings.

Discussion

Rg1 is characterized as a lesion-mimic mutant, which resembles the phenotype of HR. Previous research reported that the *Rp3* locus was tightly linked to *Rg1* (Sanz-Alferez et al. 1995). Our fine mapping results show that *Rp3*, a

Table 3 Primers for semi-quantitative RT-PCR

Gene ID	Annotion	Forward primer (5′–3′)	Reverse primer (5′–3′)	Product size (bp)
GRMZM2G054559	Phospholipase D (PLD)	AGCGAGGAGGACGAGACGA	CACCTGTGCGGCTCATAGTTC	667
GRMZM2G009479	Lipoxygenase (LOX)	GCCATCCGCAGCATCGT	CCGCCGCTCATGTGCTT	272
GRMZM2G051921	Chitinase	ATGGCTATGGCAAACTCGG	TGTTCTTGTTGACCTCGCTGAC	472
GRMZM2G017629	Jasmonate-induced protein (JIP)	CTGGTCTTGGCTACTGCTTCACTGG	TGATTCACTTCATTTGCATCCGTCC	665
GRMZM2G085967	Peroxidase 3	CACCCACTTCCACGACTGCT	GGCGAGGTTGAGGCTCTTGT	364
GRMZM2G028393[a]	Maize proteinase inhibitor (MPI)	ACAACCAGCAGTGCAACAAG	GAAGATGCGGACACGGTTAG	370
GRMZM2G156632[a]	Wound-induced serine protease inhibitor (WIP1)	TGCTGATCCTGTGCCTCCAG	CTCTCTGATCTAGCACTTGGGG	294
Internal standard	Actin	TCACCCTGTGCTGCTGACCG	GAACCGTGTGGCTCACACCA	278

[a] These two primers came from previous studies (Chintamanani et al. 2010; Feng et al. 2007)

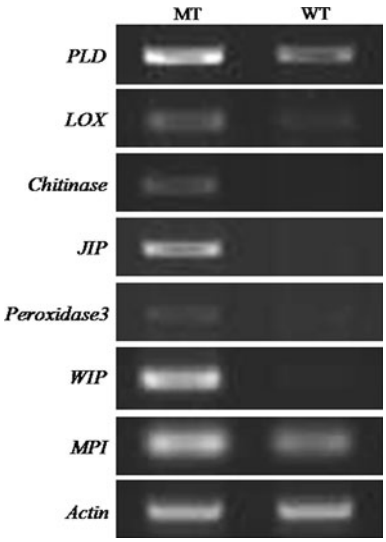

Fig. 3 Semi-quantitative RT-PCR analysis of seven defense-responsive genes in *Rg1* leaves and its wild-type siblings. *MT* heterozygous *Rg1* plants, *WT* wild-type plants

resistant (R) allele, probably underlines the phenotype of *Rg1*. Therefore, *Rg1* is likely an aberrant *Rp3* allele. In many lesion-mimic mutants, the phenotype is controlled by the aberrant R gene. In maize, another mutant *Rp1-D21* with disease lesion mimicry was caused by mutation in the rust resistance gene *rp1* (Hu et al. 1996). Additionally, some mutant R genes also have been cloned in *Arabidopsis*, rice, and barley; these abnormal R genes cause the phenotype of lesion mimicry (Büschges et al. 1997; Shirano 2002; Tang et al. 2011).

The results of transcriptome sequencing indicate that a number of genes involved in the production of ROS are over-represented in *Rg1* leaves. It has been reported that *NADPH oxidase*, *peroxidase,* and *polyamine oxidase* are implicated in the production of ROS, including hydrogen peroxide through the so-called oxidative burst processes (Apel and Hirt 2004; Foreman et al. 2003; Yoda et al. 2003). The production of ROS is one of the earliest responses to pathogen attack that occurred during HR. ROS subsequently activate the plant defense system (Bindschedler et al. 2006). H_2O_2 had been reported to play a key role in antifungal activity, synthesis of defense-related proteins, cell wall reinforcement, and induction of HR (Lanubile et al. 2011; Levine et al. 1994). The result of the over-representation of these ROS production enzymes (*NADPH oxidase*, *peroxidase* and *polyamine oxidase*) in *Rg1* leaves is consistent with our results of DAB and trypan blue staining, which suggests the production of H_2O_2 in *Rg1* leaves. Our result indicated that the aberrant *Rp3* allele in *Rg1* elicits the accumulation of ROS, which then leads to the formation of HR.

ROS are key points in response to pathogen attack. In addition to acting as a toxic molecular, ROS can also induce the expression of defense-related genes and the production of antibacterial compounds (Greenberg et al. 1994; Mittler et al. 2004; Torres et al. 2006). It has been reported that a set of genes encoding defense-related proteins such as *proteinase inhibitor*, *chitinase*, and *glucanase* are frequently induced by pathogen infection (Molina et al. 1993; Seevers et al. 1971; Sels et al. 2008; Shrestha et al. 2008). Chitinase and glucanase mainly participate in the degradation of fungal and bacterial cell walls (Kombrink et al. 1988), while proteinase inhibitors effectively inhibit the activity of proteinase produced by phytopathogenic microorganisms (Kim et al. 2009). It has been reported that over-expression of the rust disease-resistance gene *Lr10* in transgenic wheat plants confers enhanced resistance to leaf rust (Feuillet et al. 2003). Greatly up-regulated expression of two dehydrin genes in *Rg1* leaves, which have been reported to be involved in abiotic stress, supports the notion of crosstalk between abiotic and biotic stress responses (Fujita et al. 2006). The phenylpropanoid pathway, which produces phenylpropanoids responsible for various biotic

stresses, is a complex network of enzymatic reactions (Heldt 1997; Ramos-Onsins et al. 2008). Many phenylpropanoids are classified as phytoalexins synthesized in response to pathogen attack (Dixon and Paiva 1995; Naoumkina et al. 2010).

Generally, *R* gene products can recognize the avirulent pathogens, eliciting the ROS accumulation, which correlates with disease resistance (Torres et al. 2006). But some mutations in *R* genes have been found to be independent of avirulent proteins for activation (Zhang et al. 2003; Chintamanani et al. 2010). Our results of the DAB staining and transcriptome sequencing suggest that *Rg1* elicits the accumulation of ROS, which triggers the up-regulation of defense-related genes and the production of antimicrobial compounds independent of pathogens.

In conclusion, we have further characterized the *Rg1* mutant and fine mapped *Rg1* to a locus about 17 kb in the B73 genome, which harbors only one gene (*rp3*), but the corresponding region in *Rg1* was probably at least 50 kb, which is likely composed of multiple *Rp3* alleles. *Rg1* leaves stained with 3′,3′-diaminobenzidine and trypan blue suggested that *Rg1* mutant had undergone HR. Comparing the data of transcriptome sequencing of *Rg1* leaves with the control, 441genes significantly up-regulated are over-represented. These up-regulated genes included genes related to the production of ROS, defense response, and antimicrobial compounds. Our results suggest that *Rg1* induces the accumulation of ROS independent of avirulent pathogens, triggering the up-regulation of defense-related genes, the production of antimicrobial compounds, and the formation of HR. Our study provides important information, which will be useful for the eventual cloning of *Rg1* and the mechanistic understanding of this lesion-mimic locus.

Acknowledgments The research was supported by the National Basic Research Program of China (973 Program, 2009CB11840).

References

Apel K, Hirt H (2004) Reactive oxygen species: metabolism, oxidative stress, and signal transduction. Annu Rev Plant Biol 55:373–399

Bindschedler LV, Dewdney J, Blee KA, Stone JM, Asai T, Plotnikov J, Denoux C, Hayes T, Gerrish C, Davies DR (2006) Peroxidase-dependent apoplastic oxidative burst in *Arabidopsis* required for pathogen resistance. Plant J 47:851–863

Bongard-Pierce DK, Evans M, Poethig RS (1996) Heteroblastic features of leaf anatomy in maize and their genetic regulation. Int J Plant Sci 157:331–340

Bowling SA, Clarke JD, Liu Y, Klessig DF, Dong X (1997) The*cpr5* mutant of Arabidopsis expresses both NPR1-dependent and NPR1-independent resistance. Plant Cell 9:1573–1584

Brink RA, Senn PH (1931) Heritable characters in maize. XL. *Ragged*, a dominant character, linked with *A1Ts4* and *D1*. J Hered 22:155–161

Büschges R, Hollricher K, Panstruga R, Simons G, Wolter M, Frijters A, van Daelen R, van der Lee T, Diergaarde P, Groenendijk J (1997) The barley *Mlo* gene: a novel control element of plant pathogen resistance. Cell 88:695–705

Chintamanani S, Hulbert SH, Johal GS, Balint-Kurti PJ (2010) Identification of a maize locus that modulates the hypersensitive defense response, using mutant-assisted gene identification and characterization. Genetics 184:813–825

Daudi A, Cheng Z, O'Brien JA, Mammarella N, Khan S, Ausubel FM, Bolwell GP (2012) The apoplastic oxidative burst peroxidase in *Arabidopsis* is a major component of pattern-triggered immunity. Plant Cell 24:275–287

Dietrich RA, Delaney TP, Uknes SJ, Ward ER, Ryals JA, Dangl JL (1994) *Arabidopsis* mutants simulating disease resistance response. Cell 77:565–577

Dixon RA, Paiva NL (1995) Stress-induced phenylpropanoid metabolism. Plant Cell 7:1085–1097

Farkhari M, Lu Y, Shah T, Zhang S, Naghavi MR, Rong T, Xu Y (2011) Recombination frequency variation in maize as revealed by genomewide single-nucleotide polymorphisms. Plant Breeding 130:533–539

Feng YJ, Wang JW, Luo SM (2007) Effects of exogenous jasmonic acid on concentrations of direct-defense chemicals and expression of related genes in bt (*Bacillus thuringiensis*) corn (*Zea mays*). Agric Sci in China 6:1456–1462

Feuillet C, Travella S, Stein N, Albar L, Nublat A, Keller B (2003) Map-based isolation of the leaf rust disease resistance gene *Lr10* from the hexaploid wheat (*Triticumaestivum L.*) genome. Proc NatI Acad Sci USA 100:15253–15258

Foreman J, Demidchik V, Bothwell JHF, Mylona P, Miedema H, Torres MA, Linstead P, Costa S, Brownlee C, Jones JDG (2003) Reactive oxygen species produced by NADPH oxidase regulate plant cell growth. Nature 422:442–446

Fujita M, Fujita Y, Noutoshi Y, Takahashi F, Narusaka Y, Yamaguchi-Shinozaki K, Shinozaki K (2006) Crosstalk between abiotic and biotic stress responses: a current view from the points of convergence in the stress signaling networks. CurrOpin Plant Biol 9:436–442

Gray J, Close PS, Briggs SP, Johal GS (1997) A novel suppressor of cell death in plants encoded by the *Lls1* gene of maize. Cell 89:25–31

Greenberg JT, Ausubel FM (1993) Arabidopsis mutants compromised for the control of cellular damage during pathogenesis and aging. Plant J 4:327–341

Greenberg JT, Guo A, Klessig DF, Ausubel FM (1994) Programmed cell death in plants: a pathogen-triggered response activated coordinately with multiple defense functions. Cell 77:551–563

Heldt H-W (1997) Plant Biochemistry and Molecular Biology. Oxford University Press, New York

Hoisington DA, Neuffer MG, Walbot V (1982) Disease lesion mimics in maize I. effect of genetic background, temperature, developmental age, and wounding on necrotic spot formation with Les1. DevBiol 93:381–388

Hu G, Richter TE, Hulbert SH, Pryor T (1996) Disease lesion mimicry caused by mutations in the rust resistance gene *rp1*. Plant Cell 8:1367–1376

Hu G, Yalpani N, Briggs SP, Johal GS (1998) A porphyrin pathway impairment is responsible for the phenotype of a dominant disease lesion mimic mutant of maize. Plant Cell 10:1095–1106

Johal GS, Hulbert SH, Briggs SP (1995) Disease lesion mimics of maize: a model for cell death in plants. BioEssays 17:685–692

Kawano T (2003) Roles of the reactive oxygen species-generating peroxidase reactions in plant defense and growth induction. Plant Cell Rep 21:829–837

Kim JY, Park SC, Hwang I, Cheong H, Nah JW, Hahm KS, Park Y (2009) Protease inhibitors from plants with antimicrobial activity. Int J MolSci 10:2860–2872

Kombrink E, Schröder M, Hahlbrock K (1988) Several "pathogenesis-related" proteins in potato are1, 3-β-glucanases and chitinases. Proc NatI Acad Sci USA 85:782–786

Lanubile A, Bernardi J, Marocco A, Logrieco A, Paciolla C (2011) Differential activation of defense genes and enzymes in maize genotypes with contrasting levels of resistance to *Fusariumverticillioides*. EnvironExp Bot 78:39–46

Levine A, Tenhaken R, Dixon R, Lamb C (1994) H_2O_2 from the oxidative burst orchestrates the plant hypersensitive disease resistance response. Cell 79:583–593

Li T, Bai G (2009) Lesion mimic associates with adult plant resistance to leaf rust infection in wheat. Theoret Appl Genet 119:13–21

Li Q, Wan JM (2005) SSRHunter: development of a local searching software for SSR sites. Hereditas 27:808–810

Li AL, Wang ML, Zhou RH, Kong XY, Huo NX, Wang WS, Jia JZ (2005) Comparative analysis of early H_2O_2 accumulation in compatible and incompatible wheat powdery mildew interactions. Plant Pathol 54:308–316

Lorrain S, Vailleau F, Balagué C, Roby D (2003) Lesion mimic mutants: keys for deciphering cell death and defense pathways in plants? Trends Plant Sci 8:263–271

Mericle LW (1950) The developmental genetics of the *Rg* mutant in maize. Am J Bot 37:100–116

Mittler R, Vanderauwera S, Gollery M, Van Breusegem F (2004) Reactive oxygen gene network of plants. Trends Plant Sci 9:490–498

Molina A, Segura A, Garcia-Olmedo F (1993) Lipid transfer proteins (nsLTPs) from barley and maize leaves are potent inhibitors of bacterial and fungal plant pathogens. FebsLett 316:119–122

Mori M, Tomita C, Sugimoto K, Hasegawa M, Hayashi N, Dubouzet JG, Ochiai H, Sekimoto H, Hirochika H, Kikuchi S (2007) Isolation and molecular characterization of a *Spotted leaf 18* mutant by modified activation-tagging in rice. Plant Mol Biol 63:847–860

Naoumkina MA, Zhao Q, Gallego-Giraldo L, Dai X, Zhao PX, Dixon RA (2010) Genome-wide analysis of phenylpropanoid defence pathways. Molecular plant pathology 11:829–846

Qiao Y, Jiang W, Lee JH, Park BS, Choi MS, Piao R, Woo MO, Roh JH, Han L, Paek NC (2010) *SPL28* encodes a clathrin-associated adaptor protein complex 1, medium subunit μ1 (AP1M1) and is responsible for spotted leaf and early senescence in rice (*Oryza sativa*). New Phytol 185:258–274

Ramos-Onsins SE, Puerma E, Balañá-Alcaide D, Salguero D, Aguadé M (2008) Multilocus analysis of variation using a large empirical data set: phenylpropanoid pathway genes in *Arabidopsis thaliana*. Mol Ecol 17(5):1211–1223

Rohrmeier T, Lehle L (1993) *WIP1*, a wound-inducible gene from maize with homology to Bowman–Birk proteinase inhibitors. Plant Mol Biol 22:783–792

Rostoks N, Schmierer D, Mudie S, Drader T, Brueggeman R, Caldwell DG, Waugh R, Kleinhofs A (2006) Barley necrotic locus *nec1* encodes the cyclic nucleotide-gated ion channel 4 homologous to the *Arabidopsis* HLM1. Mol Genet Genomics 275:159–168

Saghai-Maroof MA, Soliman KM, Jorgensen RA, Allard RW (1984) Ribosomal DNA spacer-length polymorphisms in barley: Mendelian inheritance, chromosomal location, and population dynamics. ProcNatIAcadSci 81:8014–8018

Sandhu SS, Mazzafera P, Azini LE, Bastos CR, Colombo CA (2007) Lipoxygenase activity in Brazilian rice cultivars with variable resistance to leaf blast disease. Bragantia 66:27–30

Sanz-Alferez S, Richter TE, Hulbert SH, Bennetzen JL (1995) The *Rp3* disease resistance gene of maize: mapping and characterization of introgressed alleles. Theoret Appl Genet 91:25–32

Schweizer P, Buchala A, Silverman P, Seskar M, Raskin I, Metraux JP (1997) Jasmonate-inducible genes are activated in rice by pathogen attack without a concomitant increase in endogenous jasmonic acid levels. Plant Physiol 114:79–88

Sebela M, Radová A, Angelini R, Tavladoraki P, Frébort I, Peè P (2001) FAD-containing polyamine oxidases: a timely challenge for researchers in biochemistry and physiology of plants. Plant Sci 160:197–207

Seevers PM, Daly JM, Catedral FF (1971) The role of peroxidase isozymes in resistance to wheat stem rust disease. Plant Physiol 48:353–360

Sels J, Mathys J, De Coninck B, Cammue B, De Bolle MFC (2008) Plant pathogenesis-related (PR) proteins: a focus on PR peptides. Plant Physiol Biochem 46:941–950

Shirano Y (2002) A gain-of-function mutation in an *Arabidopsis* toll Interleukin1 receptor-nucleotide binding site-leucine-rich repeat type R gene triggers defense responses and results in enhanced disease resistance. Plant Cell 14:3149–3162

Shrestha CL, Ona I, Muthukrishnan S, Mew TW (2008) Chitinase levels in rice cultivars correlate with resistance to the sheath blight pathogen *Rhizoctoniasolani*. Eur J Plant Pathol 120:69–77

Tang J, Zhu X, Wang Y, Liu L, Xu B, Li F, Fang J, Chu C (2011) Semi-dominant mutations in the CC-NB-LRR-type R gene, *NLS1*, lead to constitutive activation of defense responses in rice. Plant J 66:996–1007

Thiel T, Kota R, Grosse I, Stein N, Graner A (2004) SNP2CAPS: a SNP and INDEL analysis tool for CAPS marker development. Nucleic Acids Res 32:e5

Torres MA, Jones JDG, Dangl JL (2006) Reactive oxygen species signaling in response to pathogens. Plant Physiol 141:373–378

Van Der Luit AH, Piatti T, DoornA Van, Musgrave A, Felix G, Boller T, Munnik T (2000) Elicitation of suspension-cultured tomato cells triggers the formation of phosphatidic acid and diacylglycerol pyrophosphate. Plant Physiol 123:1507–1516

Webb CA, Richter TE, Collins NC, Nicolas M, Trick HN, Pryor T, Hulbert SH (2002) Genetic and molecular characterization of the maize *rp3* rust resistance locus. Genetics 162:381–394

Wilkinson DR, Hooker AL (1968) Genetics of reaction to *Puccinisorghi* in ten corn inbred lines from Africa and Europe. Phytopathology 58:605–608

Wolter M, Hollricher K, Salamini F, Schulze-Lefert P (1993) The *mlo* resistance alleles to powdery mildew infection in barley trigger a developmentally controlled defence mimic phenotype. Mol Gen Genet 239:122–128

Wu C, Bordeos A, Madamba MRS, Baraoidan M, Ramos M, Wang G, Leach JE, Leung H (2008) Rice lesion mimic mutants with enhanced resistance to diseases. Mol Genet Genomics 279:605–619

Xu F, Fan C, He Y (2007) Chitinases in *Oryza sativa* ssp.*japonica* and *Arabidopsis thaliana*. J Genet Genomics 34:138–150

Yamanouchi U, Yano M, Lin H, Ashikari M, Yamada K (2002) A rice spotted leaf gene, *Spl7*, encodes a heat stress transcription factor protein. Proc NatI Acad Sci USA 99:7530–7535

Yao Q, Zhou R, Fu T, Wu W, Zhu Z, Li A, Jia J (2009) Characterization and mapping of complementary lesion-mimic genes *lm1* and *lm2* in common wheat. Theoret Appl Genet 119:1005–1012

Yin Z, Chen J, Zeng L, Goh M, Leung H, Khush GS, Wang GL (2000) Characterizing rice lesion mimic mutants and identifying a mutant with broad-spectrum resistance to rice blast and bacterial blight. Mol Plant Microbe Interact 13:869–876

Yoda H, Yamaguchi Y, Sano H (2003) Induction of hypersensitive cell death by hydrogen peroxide produced through polyamine degradation in tobacco plants. Plant Physiol 132:1973–1981

Zeng LR, Qu S, Bordeos A, Yang C, Baraoidan M, Yan H, Xie Q, Nahm BH, Leung H, Wang GL (2004) *Spotted leaf11*, a negative regulator of plant cell death and defense, encodes a U-box/armadillo repeat protein endowed with E3 ubiquitin ligase activity. Plant Cell 16:2795–2808

Zhang Y, Goritschnig S, Dong X, Li X (2003) A gain-of-function mutation in a plant disease resistance gene leads to constitutive activation of downstream signal transduction pathways in *suppressor of npr1-1*, *constitutive 1*. Plant Cell 15:2636–2646